ORIGINAL ARTICLE

Co-immunization with L-Myc enhances CD8+ or CD103+ DCs mediated tumor-specific multi-functional CD8+ T cell responses

Dafei Chai[1,2,3] | Zichun Zhang[1,4] | Nan Jiang[1,4] | Jiage Ding[1,3] | Dong Qiu[4] |
Shang Yuchen Shi[5] | Gang Wang[1,2,3] (iD) | Lin Fang[1,2,3] | Huizhong Li[1,2,3] | Hui Tian[1,2,3] |
Jie Yang[1,2,3] | Qing Zhang[1,2,3] | Junnian Zheng[2,3] (iD)

[1]Cancer Institute, Xuzhou Medical University, Xuzhou, China

[2]Jiangsu Center for the Collaboration and Innovation of Cancer Biotherapy, Cancer Institute, Xuzhou Medical University, Xuzhou, China

[3]Center of Clinical Oncology, Affiliated Hospital of Xuzhou Medical University, Xuzhou, China

[4]Department of Urology, Affiliated Hospital of Xuzhou Medical University, Xuzhou, China

[5]Department of Radiation Oncology, Affiliated Hospital of Xuzhou Medical University, Xuzhou, China

Correspondence
Junnian Zheng, Cancer Institute, Xuzhou Medical University, 84 West Huaihai Road, Xuzhou, Jiangsu 221002, China.
Email: jnzheng@xzhmu.edu.cn

Funding information
Youth Technology Innovation Team of Xuzhou Medical University, Grant/Award Number: TD202003; National Natural Science Foundation of China, Grant/Award Number: 82072814 and 81871869; Natural Science Foundation of Jiangsu Province, Grant/Award Number: BK20190986; Key Research Development project of Xuzhou (Industry Foresight and Common Key Technology), Grant/Award Number: KC19082; Qing Lan Project of Jiangsu Province

Abstract

Renal carcinoma shows a high risk of invasion and metastasis without effective treatment. Herein, we developed a chitosan (CS) nanoparticle-mediated DNA vaccine containing an activated factor L-Myc and a tumor-specific antigen CAIX for renal carcinoma treatment. The subcutaneous tumor models were intramuscularly immunized with CS-pL-Myc/pCAIX or control vaccine, respectively. Compared with single immunization group, the tumor growth was significantly suppressed in CS-pL-Myc/pCAIX co-immunization group. The increased proportion and mature of CD11c+ DCs, CD8+CD11c+ DCs and CD103+CD11c+ DCs were observed in the splenocytes from CS-pL-Myc/pCAIX co-immunized mice. Furthermore, the enhanced antigen-specific CD8+ T lymphocyte proliferation, cytotoxic T lymphocyte (CTL) responses, and multi-functional CD8+ T cell induction were detected in CS-pL-Myc/pCAIX co-immunization group compared with CS-pCAIX immunization group. Of note, the depletion of CD8 T cells resulted in the reduction of CD8+ T cells or CD8+CD11c+ DCs and the loss of anti-tumor efficacy induced by CS-pL-Myc/pCAIX vaccine, suggesting the therapeutic efficacy of the vaccine was required for CD8+ DCs and CD103+ DCs mediated CD8+ T cells responses. Likewise, CS-pL-Myc/pCAIX co-immunization also significantly inhibited the lung metastasis of renal carcinoma models accompanied with the increased induction of multi-functional CD8+ T cell responses. Therefore, these results indicated that CS-pL-Myc/pCAIX vaccine could effectively induce CD8+ DCs and CD103+ DCs mediated tumor-specific multi-functional CD8+ T cell responses and exert the anti-tumor efficacy. This vaccine strategy offers a potential and promising approach for solid or metastatic tumor treatment.

1 | INTRODUCTION

Renal cell carcinoma (RCC) accounts for 90% of malignant neoplasms arising in the kidney in adults.[1] The malignant degree of RCC is very high and not easy to find early.[2] As an immunogenic tumor, RCC treated with immunotherapy has shown spontaneous, partial or complete remission, which dues to improve the responses of the immune system against tumor cells.[3] Although the development of molecular targeted therapies such as PD-L1 or CTLA-4 inhibitors was made in recent years, metastatic renal carcinoma is still considered incurable for the low five-year survival rate.[4] The recent clinical application of CAR-T or immune checkpoint inhibitors can effectively inhibit tumor development, but the efficacy against solid tumors is still not satisfactory.[5,6] Thus, there is an urgent need for new therapeutic strategies that could specifically eliminate tumor and induce long lasting protection.

As an essential part of immunotherapy for tumor, DNA vaccination is a promising approach for activating CD8^{+} T cell responses.[7,8] As the plasmid DNA is injected intramuscularly, the encoding antigen can be expressed in human body and induce a cellular and humoral immune response.[9] CAIX protein, whose 38-414 amino acid form extracellular domain, is an isomer of the carbonic anhydrase enzyme family.[10] The human CAIX (hCAIX) gene inducing a malignant phenotype is expressed in the majority of renal carcinoma, but not in normal renal tissues or only a small amount of hCAIX expression in gastric mucosa and bile duct epithelial cells.[11,12] Therefore, CAIX is used as a potential target for renal carcinoma immunotherapy.[13] Recent years, various vaccines based CAIX antigen have been manufactured for tumor immunotherapy.[14,15] We and others had demonstrated CAIX-based DNA vaccine could induce antigen-specific CD8^{+} T cell immune response with the help of adjuvant, and inhibit the tumor growth of renal carcinoma.[16-18] But the challenges of its effectiveness and safety remain huge in clinical application in the future.

CAIX antigen is a 20 kDa protein, and possesses several naturally processing epitopes, including cytotoxic lymphocyte (CTL), and T-helper cell recognition sites, but the immunogenicity of alone CAIX is too weak to activate lasting and effective immune responses.[19] Therefore, the DNA of encoded cytokines, transcription factors or bacterial proteins, etc, is served as the adjuvant, which can effectively improve DNA vaccine immunogenicity and cause a strong immune response.[20] L-Myc is a member of Myc gene family that is the important regulatory factors in tumor development.[21] L-Myc is selectively expressed in common dendritic cells (DCs) progenitor during DC development of the immune system. Mature DCs can maintain.

L-Myc expression even in the presence of inflammatory signals, but lack expression of c-Myc and N-Myc. The study has demonstrated that the significantly reduced migratory CD103^{+} conventional DCs

are found in the lung and liver tissues from L-Myc-deficient mice.[22] Importantly, loss of L-Myc by DCs results in a significant decrease activation of T cells during infection by vesicular stomatitis virus and Listeria monocytogenes.[22] Therefore, L-Myc as an immune cell regulator, its expression and transcriptional activity enhancement in ordinary DCs progenitor cells and pre-cDCs, especially in CD8α^{+} cDCs and CD103^{+} cDCs, are essential for enhancing T cell immune responses. L-Myc might be used as a DNA vaccine adjuvant that enhances DCs-mediating T cell immune responses.

It is critical for enhancing the induction of antigen-specific immune responses to effectively deliver DNA vaccine into the host.[23] Chitosan (CS) is a deacetylated derivative of chitin with completely non-toxic, biocompatible and biodegradable nanomaterial.[24] The cationic nature of primary amines of CS can effectively promote the binding and protection of DNA of intracellular delivery.[25] The DNA of targeting antigen encapsulated in CS can effectively induce a mucosal immune response or systemic immune response with high safety.[26] Therefore, CS nanoparticle-based delivery system might enhance the therapeutic effect of DNA vaccine.

In this study, we determine whether L-Myc could enhance the therapeutic efficacy of CAIX vaccine in primary or metastasis models. Our results suggested that L-Myc could be a novel adjuvant to enhance the CAIX vaccine-induced CTL responses and multi-functional CD8^{+} T cell responses in hCAIX-Renca bearing mice or lung metastasis models. This vaccine strategy provides a universal applicability reference for the development of therapeutic tumor vaccines.

2 | MATERIALS AND METHODS

2.1 | Plasmid construction

Murine L-Myc DNA fragment was generated by using the synthetic gene coding region (Biotechnology Co., Ltd) and cloned into the HindIII and XbaI sites of pcDNA3.1 vector to obtain plasmid L-Myc (pL-Myc). pL-Myc was sequenced to confirm that the plasmid was successfully constructed. The plasmid pcDNA3.1-CAIX (pCAIX) has been constructed previously.[16] The plasmids were transformed into DH5α competent cells, propagated in LB broth supplemented with 100 μg/mL ampicillin, and purified from DH5α grown overnight using Endo-Free Plasmid Mega Kit (Qiagen).

2.2 | Preparation of CS-DNA nanocomplex

The plasmid DNA was encapsulated with CS (Sigma-Aldrich, Merk) according to a previously described method.[27] Briefly, plasmid DNA were dissolved in 25 mM Na_2SO_4 solution to a final concentration of

0.5 mg/mL, and CS was dissolved in sodium acetate buffer (pH 5.5) to a final concentration of 1 mg/mL. Then, DNA-Na$_2$SO$_4$ solution was mixed with an equal volume of CS solution at 55°C water bathing. Mixed solutions were vortexed instantly 1 minute and incubated at room temperature for 30 minutes to allow complex formation, then centrifuged at 12 000g for 5 minutes. Took the supernatant to measure the DNA quality, calculated the encapsulation efficiency, and frozen the pellet for use.

2.3 | Particle size and zeta potential analysis

By dynamic light scattering (DLS), nanoparticle size measurements were conducted using the Zetasizer Nano ZS (Malvern, Southborough, MA, USA). Briefly, the nanoparticles were suspended in ddH$_2$O at a concentration of 1 mg/ml. The size measurements were performed at 25°C and at a 173° scattering angle. The mean hydrodynamic diameter was determined by cumulative analysis. The zeta potential determinations based on the electrophoretic mobility of the nanoparticles in the aqueous medium were performed by the Zetasizer Nano ZS using folded capillary cells in automatic mode.

For the morphology, the nanoparticles were resuspended in ddH$_2$O and deposited onto a glow discharged carbon-coated 400 square mesh copper grid. Subsequently, the samples were negatively stained with 1 wt% uranyl acetate. A few seconds after staining, the copper mesh was dried with filter paper and detected by transmission electron microscopy (TEM).

2.4 | Gel retardation assay

The integrity of CS-DNA was assayed to investigate the stability of the plasmid inside. The naked plasmid pcDNA3.1 was used as a control, and the mass ratios of CS and DNA (CS-DNA) were 5:1, 2:1, 1:1, 0.5:1, 0.25:1 and 0.125:1 as experimental well. The amount of DNA used is 1 μg/well. All samples were packed onto a gel containing 1% agarose and ran in l × TE buffer (pH 8.3) on a gel electrophoresis system (Mupid-One, Takara). The gel was then analyzed at a wavelength of 312 running under gel imaging system (FireReader).

2.5 | Cell lines and cell culture

Human embryonic kidney cell line (HEK293T) was obtained from the American Type Culture Collection (ATCC), and murine renal cancer cell line (Renca) was purchased from Cobioer Biosciences. These cells were passed the certificate of analysis. HEK293T cells were cultured in DMEM medium containing 10% fetal bovine serum (FBS; ExCell Bio), 100 U/mL penicillin, and 100 μg/mL streptomycin in a 5% CO$_2$ atmosphere at 37°C. Renca cells were cultured in RPMI 1640 medium supplemented with 10% FBS, 100 U/mL penicillin and 100 μg/mL streptomycin, 2 mM L-glutamine, 1 × MEM non-essential amino acid solution, 1 mM sodium pyruvate solution. The CAIX

lentivirus produced by HEK293T was used to infect Renca cells to establish the stable over-expressing hCAIX-Renca cells according to the previous method.[16]

2.6 | Animal models and vaccine treatment

Six-week old female BALB/c mice were purchased from Vital River Laboratory (Beijing, China) and remained in the pathogen-free conditions. All animal procedures and protocols are approved by the Experimental Animal Ethics Committee of Xuzhou Medical University, and implemented in accordance with the Xuzhou Medical University Laboratory Animal Care and Use Guide.

In the subcutaneous tumor-bearing mice, one week after subcutaneous injection of 5×10^5 hCAIX-Renca cells, mice were randomly divided into four groups (n = 5 each group) and anesthetized with 1% isoflurane. The anesthetized mice were intramuscularly immunized with mock (CS-pcDNA3.1), CS-pL-Myc or CS-pCAIX vaccine at a dose of 50 μg each plasmid, and CS-pL-Myc/pCAIX at a dose of 100 μg. For Mock, CS-pL-Myc or CS-pCAIX vaccine immunized group, mice received additional 50 μg mock vaccine to ensure that the total DNA amount was 100 μg. The mice were given an immunity boost on the 10th and 20th days after the initial vaccination. Size of tumor was measured twice at every week. Tumor volume was evaluated by the formula V (mm^3) = (length × width^2)/2. Mice were sacrificed by cervical dislocation on day 42 after tumor inoculation and tumor tissues were taken out and weighed.

For establishing the tumor lung metastasis models, 1×10^6 hCAIX-Renca cells were injected through the tail vein at day 0. The anesthetized mice were intramuscularly injected with each vaccine at day −10, and repeated immunization at day 0 and day 10 post tumor inoculation. 28 days after tumor inoculation, the mice were sacrificed and metastatic nodules were quantified in lung tissues.

2.7 | Western blotting

The samples were collected and dissolved in RIPA lysis buffer (Beyotime) supplemented with PMSF (Invitrogen). The same quality protein samples were added loading buffer and heating at 100°C for 5 minutes, then separated by 10% SDS-PAGE and electro-blotted onto a polyvinylidene difluoride PVDF membrane (Millipore). The membrane was blocked with 5% BSA solution and and incubated with anti-L-Myc (Abcam) or anti-CAIX primary antibody (Abcam) at 4°C overnight. Subsequently, membranes were washed with Tris-buffered saline with 0.1% Tween 20 (TBST) and incubated with HRP-linked secondary antibody at room temperature for 2 hours. After rinsing with TBST, the enhanced chemiluminescence (ECL, Thermo Fisher Scientific) was used to detect the immunoreactive band. The density of the bands on the membrane were scanned and analyzed with an Image-J analyzer tool.

2.8 | Preparation of single cell suspension

For the acquisition of splenocytes, the tissue was gently ground in PBS buffer by using a 5 mL clean syringe plunger. The released cells were collected, resuspended and passed through 70 μm nylon mesh. After centrifugation at 1000 rpm for 5 minutes, red blood cells were lysed with ACK lysis buffer. The remaining cells were collected and resuspended in RPMI 1640 medium to prepare a single cell suspension. For the single cell suspension from tumor tissues, samples are firstly cut into small pieces, then performed grinding and digestion in serum-free medium containing 200 U/mL collagenase IV (Solarbio). Finally, the method for single cell suspension is the same as that of splenocytes. TILs are separated on a 40% Percoll (GE Healthcare) gradient.

2.9 | Flow cytometry analysis

The immune cell populations were subjected to surface staining for flow cytometry analysis. The used antibodies are as follows: PE-conjugated anti-CD3ε (Biolegend), PerCP-conjugated anti-CD4 (BD Pharmingen), PerCP-conjugated anti-CD8α (BD Pharmingen), FITC-conjugated anti-NK1.1 (Biolegend), FITC-conjugated anti-CD11b (Biolegend), PE-conjugated anti-CD103 (Biolegend), APC-conjugated anti-CD11c (BD Pharmingen), PerCP-conjugated anti-F4/80 (Biolegend), or FITC-conjugated anti-Gr-1 (Biolegend).

For analyzing cytokine secretion, splenocytes were inoculated into a 12-well plate at 4×10^6/well and incubated with 10 μg/mL CAIX protein at 37°C and 5% CO_2 for 3 days, then added 500 ng/mL Ionomycin (Sigma-Aldrich) and 50 ng/mL PMA (Sigma-Aldrich) and 5 ng/mL Brefeldin A (BFA, eBioscience) to incubate for 5 hours. Then cells were collected and operated extracellular staining with anti-mouse PerCP-conjugated anti-CD8α and intracellular staining with following anti-mouse antibodies: APC-conjugated anti-IFN-γ (BD Pharmingen), PE-conjugated anti-IL-2 (BD Pharmingen), FITC-conjugated anti-TNF-α (BD Pharmingen). The data acquired from BD FACSCanto II (BD Biosciences) in FACSDiva software were analyzed by FlowJo software (Tree Star Inc).

2.10 | CD8 T cell proliferation assay

Lymphocytes were added to 48-well flat-bottomed tissue culture plates at 1×10^6 cells/well containing IL-2 (50 U/ml)and CAIX protein (10 μg/mL). The plates were cultured at 37 ˚C in a humidified incubator with 5% CO_2 for 5 days and the medium was changed medium at 3 days. Cell proliferation assay was performed using the BeyoClick™ EdU Cell Proliferation Kit with Alexa Fluor 647 (Beyotime). Briefly, the cells were incubated with 10 μM EdU for 2 hours at 37°C. Then, cells were collected and performed the surface staining with PerCP-conjugated anti-CD8α for 30 minutes. After fixation, permeabilization and rinse, the cells were exposed to 100 μL of click reaction cocktail for 30 minutes. The cells were washed three times with permeabilization buffer. The percentages of EdU⁺ cells in CD8⁺ T cells were analyzed by flow cytometry and defined as the proliferation rate.

2.11 | RTCA killing test

Lymphocytes were cultured in RPMI 1640 medium containing IL-2 (50 U/mL) and CAIX protein (10 μg/mL) for 7 days at 37°C in humidified air with 5% CO_2. The processed cells were washed and resuspended as effector cells in medium. hCAIX-Renca were used as target cells. The baseline was measured by adding the medium (50 μL/well) to RTCA plate (ACEA Biosciences). The target cells (10^4/well) were inoculated into RTCA plate. After the cells adhere, effector cells were added by the effector-target cell ratio of 50:1 and incubated for 96h. Finally, the cell index was analyzed by using RTCA analysis software (ACEA Biosciences).

2.12 | ELISPOT assay

The assay was performed by using the murine IFN-γ T cell enzyme-linked immunospot (ELISPOT) monochromatic enzyme kit (eBioscience). Briefly, ELISPOT 96-well plate was coated with the IFN-γ capture antibody provided in the kit overnight at 4°C. Discarded the antibody solution and washed the coated plate. Then the plate was blocked with RMPI1640 with 10% serum for 2 hours, and added the isolated lymphocytes (1×10^6 cells) to each well with 200 μl medium containing IL-2 (50 U/mL) and CAIX protein (10 μg/mL). After incubation for 60 hours at 37°C, the plates were processed according to the instructions of the kit, developed and read on the ImmunoSpot Series 3 analyzer (Cellular Technology).

2.13 | CD8 T cell depletion in vivo

At day −2 after administration of vaccines in the therapeutic model, mice were intraperitoneally injected the purified anti-mouse CD8α mAb (clone 53-6.7, 0.5 mg/mouse) to deplete CD8 T cells. The antibody injections were repeated on day 5 and day 12 after the first vaccination. The efficacy of cell depletion was confirmed by flow cytometric analysis of the spleens.

2.14 | Immunohistochemistry staining

The paraffin tissue sections were initially deparaffinized at 65°C for 1 hour, placed in xylene solutions I and II for further permeabilization for 5 minutes, and then dehydrated in 100%, 90%, 85%, 70% and 50% ethanol solutions. After endogenous peroxidation blocking and antigen retrieval with lemon salt buffer, the tissue section was blocked with 10% BSA, incubated with anti-mouse CD8 antibody (diluted 1:100; eBioscience) overnight at 4°C. The sections

were wash with PBS and incubated with secondary antibody, and then with streptavidin peroxidase (Zhongshan Biotechnology Co., Ltd., Beijing). The samples were developed by treatment with DAB Detection Kit (Zhongshan Biotechnology) and with hematoxylin to counter stain the nuclei. Immunostaining evaluation was performed as described before.[28]

2.15 | Pathological analyses

The sample tissues were fixed with 4% paraformaldehyde, embedded in paraffin, cut into 5 μm slices, H&E stained according to the manufacturer's instructions, and blinded by different pathologists to evaluate histopathological sections, and then the photos were taken on a Nikon SCLIPSS TE2000-S microscope (Nikon) equipped with ACT-1 software at ×200 magnification.

2.16 | Statistical analyses

Statistical significance was evaluated with GraphPad Prism Software and determined by a two-tailed unpaired Student's t test or ANNOVA as mean and standard deviation (means ±SD). The statistical p value was set as *P <.05; **P <.01; ***P <.001 for different significance levels.

3 | RESULT

3.1 | Characterization of CS-DNA nanoparticle vaccine

The plasmid DNA was encapsulated with CS to prepare the CS-DNA nanoparticles according to previously developed methods.[27] As measured by dynamic light scattering, the size intensity curves of CS-DNA nanoparticles were evenly dispersed. Z-Average sizes and surface zeta potential of the CS-DNA nanoparticles were about 223.5 nm (Figure 1A) and 12.2 mV (Figure 1B), respectively. These results suggested that the particle size of CS-DNA was suitable for immune induction, and the positive charge of CS-DNA was favorable for the particle that bonded to the cells. In the gel blocking analysis, compared with naked DNA plasmids, CS-DNA were blocked in the gel electrophoresis wells at the mass ratio (CS/DNA) exceeded 2:1 (Figure 1C), indicated that DNA could effectively encapsulate with CS strong electrical binding force. Moreover, the diameter of CS-DNA detected by electron microscope was about 200 nm (Figure 1D). Our previous study had also shown that CS nanoparticles could be used as the effective delivery system for gene expression in vitro and in vivo.[26] To confirm the expression of CS-DNA vaccines in vivo, CS-pL-Myc or CS-pCAIX were injected intramuscularly and evaluated their expression in mice. Western blot analysis indicated a higher expression of L-Myc or CAIX at a predicted molecular weight in CS-pL-Myc or CS-pCAIX-treated mice compared with control-treated

mice (Figure 1E-H). Therefore, these results indicated that CS-DNA nanoparticles could effectively promote the gene expression in vivo.

3.2 | CS-pL-Myc/pCAIX co-immunization inhibits subcutaneous tumor growth accompanied with the increased induction of DCs and CD8^{+} T cells
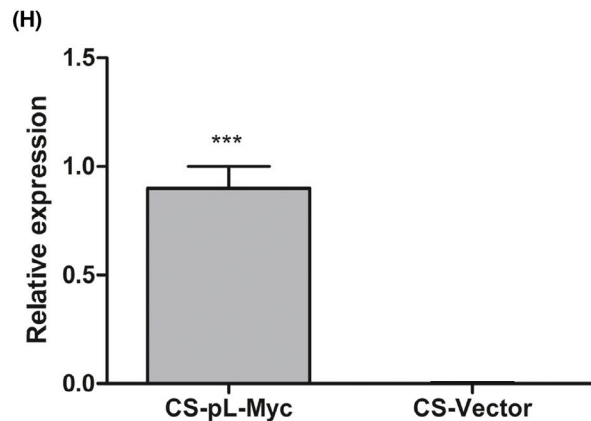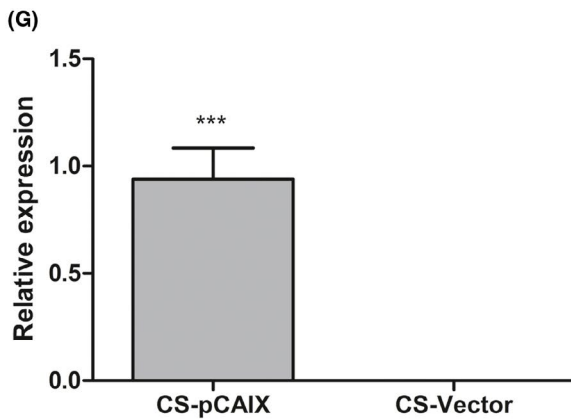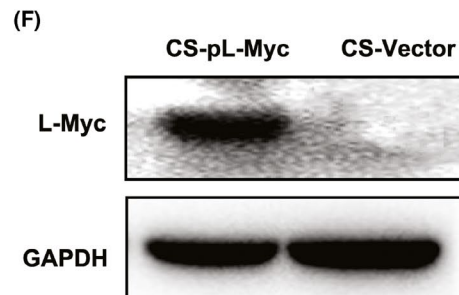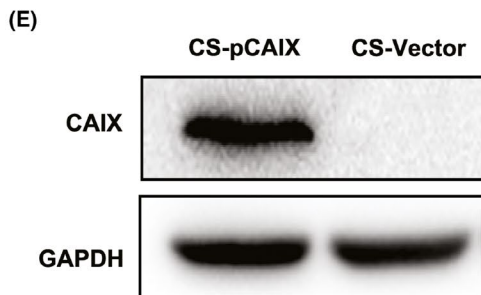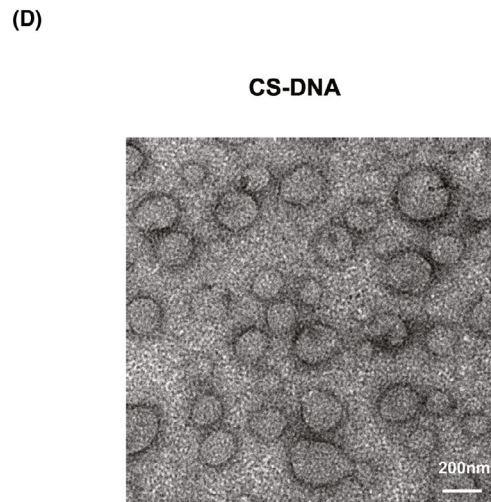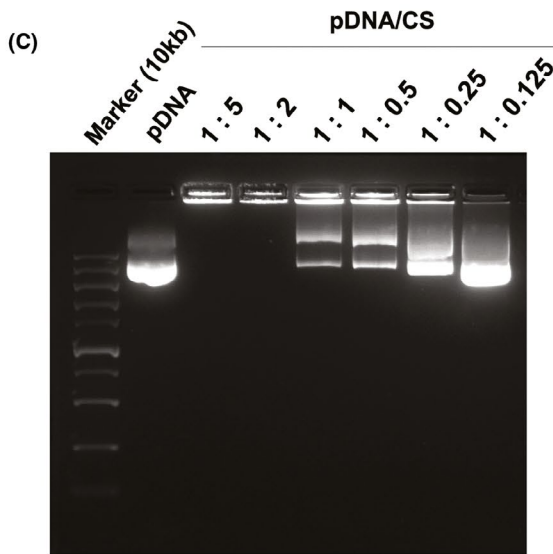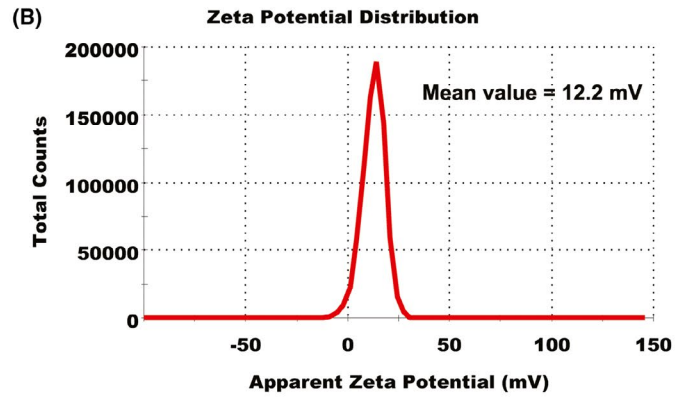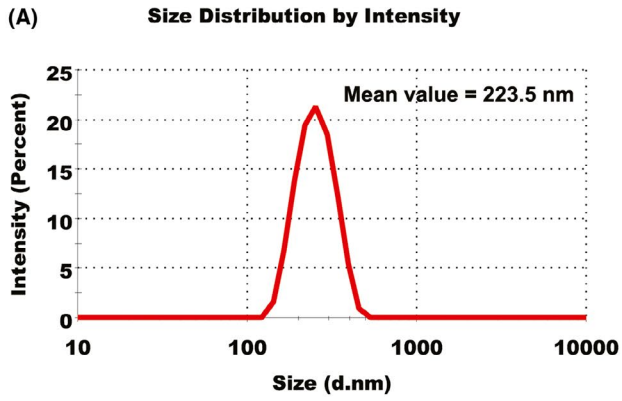
To evaluate the therapeutic effect of CS-pL-Myc/pCAIX vaccine, subcutaneous tumor models were established by inoculating with hCAIX-Renca in 6-week old BALB/c mice. Seven days after tumor inoculation, mice were intramuscularly immunized with mock, CS-pL-Myc, CS-pCAIX or CS-pL-Myc/pCAIX vaccines, respectively (Figure 2A). Compared with CS-pCAIX immunized mice, the tumor growth was significantly inhibited in CS-pL-Myc/pCAIX co-immunized mice (Figure 2B-C). The similar reduction of tumor mass was also observed in CS-pL-Myc/pCAIX co-immunization group (Figure 2D). Likewise, the survival rate of CS-pL-Myc/pCAIX treated-mice was much higher than that of CS-pCAIX-treated mice (Figure 2E). Therefore, these data indicated that CS-pL-Myc/pCAIX co-immunization could effectively suppress primary tumor growth.

To reveal the underlying anti-tumor mechanism by CS-pL-Myc/pCAIX vaccine, we firstly analyzed various immune cell components in tumor model immunized with various vaccines. The increased percentages and total numbers of T cells, DCs, and macrophages, similar NK cells, and reduced MDSCs were observed in TILs of tumor tissues from CS-pL-Myc/pCAIX co-immunization group compared with CS-pCAIX immunization group. There has no difference in CD4^{+} T cells, while the proportion and quantity of CD8^{+} T cells was significantly different (Figure 2F and G). Therefore, co-immunization with L-Myc could increase the induction of DCs, T cells, especially CD8^{+} T cells induced by CAIX vaccine and exert an anti-tumor effect in mice.

3.3 | Co-immunization with L-Myc enhances the induction and mature of CD8^{+} DCs and CD103^{+} DCs subsets

Migrating CD103^{+} DCs present the tumor antigens to the residence CD8^{+} DCs, indicating that cross-presentation of the antigen by the MHC II or MHC I antigen peptide form were performed for triggering T cell activation.[29,30] During DC maturation and activation, L-Myc is only selectively expressed in CD103^{+} or CD8^{+} DCs, and is also necessary for their stability and proliferative activity.[22] Therefore, we explored whether L-Myc as an adjuvant could enhance the anti-tumor effect of the vaccine. The percentages of DCs and DC subpopulation were detected by flow cytometry in the splenocytes of mice immunized with various vaccines (Figure 3A). The significantly enhanced percentages of CD11c^{+} DCs, CD103^{+}CD11c^{+} or CD8^{+}CD11c^{+} DCs subpopulation were observed in CS-pL-Myc/pCAIX co-immunization group compared with CS-pCAIX immunization group (Figure 3B-D). Accordingly, the increased induction of DCs subpopulation was also significantly

(A) Size Distribution by Intensity

Mean value = 223.5 nm

(B) Zeta Potential Distribution

Mean value = 12.2 mV

(C)

pDNA/CS

Marker (10kb) pDNA 1:5 1:2 1:1 1:0.5 1:0.25 1:0.125

(D)

CS-DNA

200nm

(E)

CS-pCAIX   CS-Vector

CAIX

GAPDH

(F)

CS-pL-Myc   CS-Vector

L-Myc

GAPDH

(G)

CS-pCAIX   CS-Vector

***

(H)

CS-pL-Myc   CS-Vector

***

FIGURE 1 Characterization of CS-DNA nanoparticle vaccine. (A) Size intensity curves. (B) Surface zeta potential. (C) Gel blocking analysis of CS-DNA. (D) The micrographs of CS-DNA nanoparticles were acquired by transmission electron. Scale bars, 200 nm. (E and F) The expression of L-Myc or CAIX was detected by western blot in muscular tissues from mice immunized with CS-pL-Myc or CS-pCAIX. CS-Vector was used as the corresponding control. (G and H) Quantification of L-Myc or CAIX expression by densitometry in (E) and (F). Data are from one representative experiment of three performed and presented as the mean ±SD. The different significance was set at ***P <.001

FIGURE 2 Therapeutic effects of CS-pL-Myc/pCAIX vaccine in subcutaneous hCAIX-Renca tumor model. (A) Schema of the subcutaneous hCAIX-Renca-tumor model intramuscularly inoculated with various vaccines on day 7 after tumor inoculation. (B) Tumor volume. (C) Tumor volumes. (D) Tumor weight. (E) Survival curve. (F) The frequencies of T, CD4$^+$ T, CD8$^+$ T, NK, DCs, macrophages, or MDSCs were analyzed in TIL of mice treated with vaccines. (G) Total numbers of various immune cells in (F). Data are from one representative experiment of three performed and presented as the mean ±SD. The different significance was set at *P <.05, **P <.01, and ***P <.001; ns, not significant
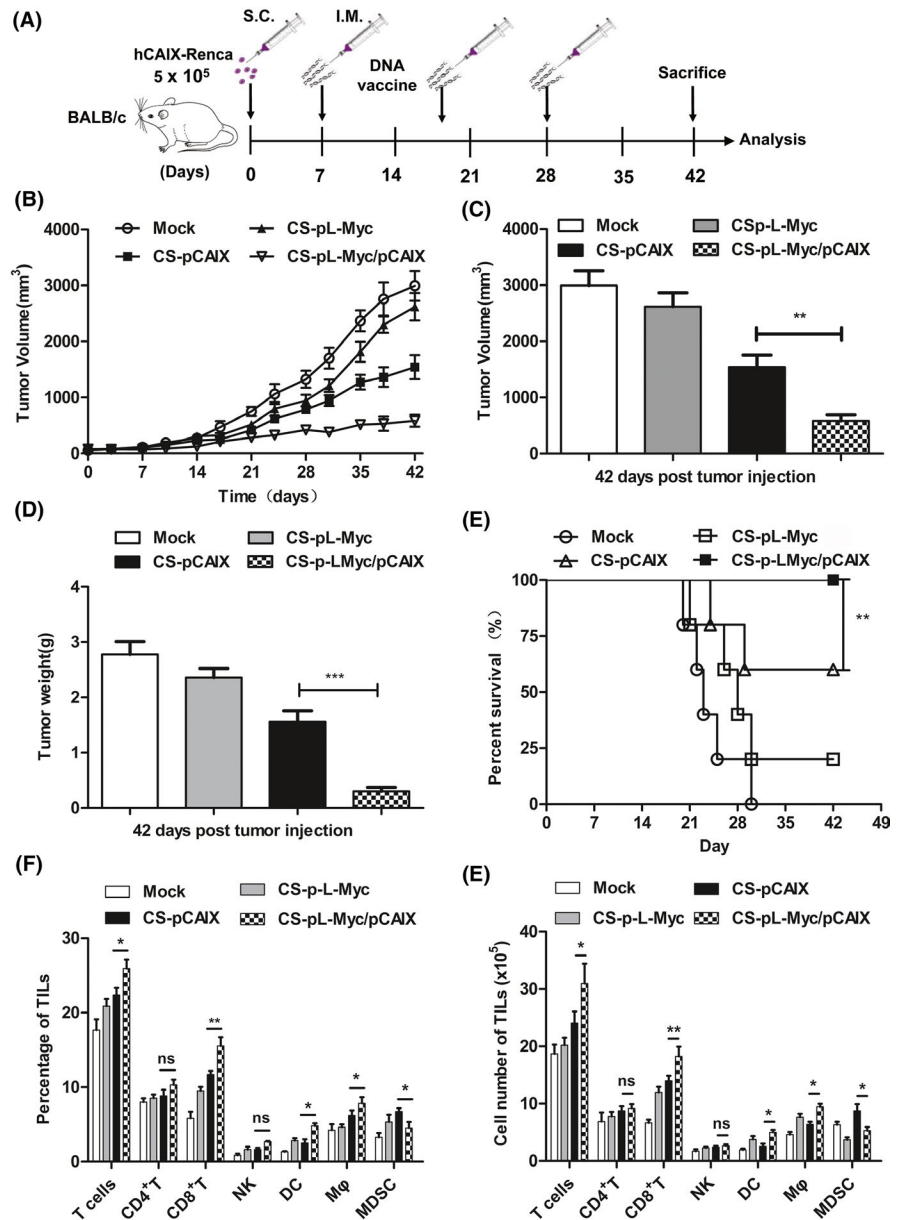
higher in CS-pL-Myc immunization group than mock immunization group (Figure 3B-D). Next, the proportion of CD80, CD86 or MHCII expression on DC cells was significantly higher in the CS-pL-Myc/pCAIX group than that in the CS-pCAIX group (Figure 3E-H), suggested that CS-pL-Myc/pCAIX co-immunization could induce the activation and mature of DCs in tumor-bearing mice. Therefore, CS-pL-Myc/pCAIX could enhance the induction and mature of CD103$^+$CD11c$^+$ or CD8$^+$CD11c$^+$DCs, implied that the vaccine promoted the uptake and processing of tumor antigens to activate CD8 T cell responses.

3.4 | CS-pL-Myc/pCAIX co-immunization induces antigen-specific multi-functional CD8$^+$ T cell immune responses

To evaluate CS-pL-Myc/pCAIX mediated anti-tumor immunity, CD8 T cell immune responses were assessed in various vaccine immunization groups. CS-pL-Myc/pCAIX group showed a higher proliferation of CD8 T cells than CS-pCAIX group (Figure 4A). CS-pL-Myc/pCAIX co-immunized mice exhibited a stronger tumor killing ability than those from CS-pCAIX immunized mice (Figure 4B). Furthermore,
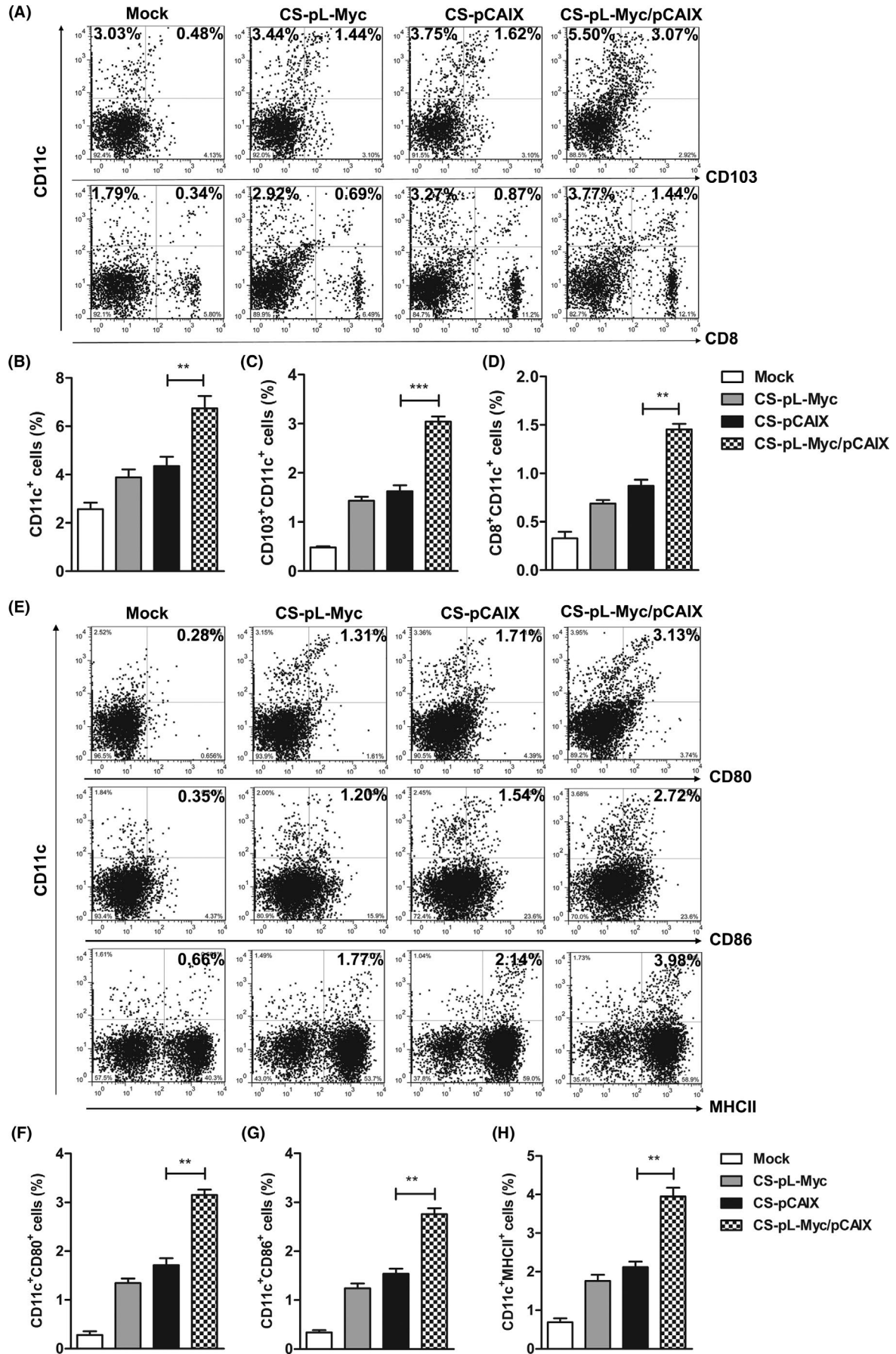
FIGURE 3 Co-immunization with L-Myc enhances the induction and mature of DC subsets. Mice immunized with vaccines were sacrificed on the 42 days post tumor inoculation, the proportions of DCs subsets were analyzed by flow cytometry in spleen. (A) The representative flow cytometry of CD11c$^+$, CD103$^+$CD11c$^+$ or CD8$^+$CD11c$^+$ DCs subpopulation. (B-D) Statistical analysis of the percentages of DCs subsets in (A). (E) The expression of CD80, CD86, or MHC-II on CD11c$^+$ cells. (F-H) Statistical analysis of the frequencies of CD11c$^+$CD80$^+$, CD11c$^+$CD86$^+$ or CD11c$^+$MHC II$^+$ cells in (E). The data shown are the representative of three experiments. Data are means ±SD. The different significance was set at**P <.01, ***P <.001

the dramatically induction of IFN-γ-producing T cells detected by ELISPOT assay were found in CS-pL-Myc/pCAIX co-immunization group (Figure 4C and D). By intracellular staining and flow cytometry analysis, we also observed the increased percentages of secreting IFN-γ, TNF-α or IL-2 CD8$^+$T cells in the CS-pL-Myc/pCAIX vaccine group (Figure 4E and F). These results indicated that CS-pL-Myc/pCAIX co-immunization could enhance the induction of tumor antigen-specific CD8$^+$ T cell responses.

It is important that the multi-functional CD8 T cells play a key role for the effect of protective immunity by secreting various cytokines.[31] Therefore, the induction of antigen-specific multi-functional CD8$^+$ T cells was detected in the spleen or tumor of tumor-bearing mice treated with various vaccines. As shown in Figure 5A-H, CS-pL-Myc/pCAIX treated mice showed the raised frequency of CD8$^+$ T with two markers (TNF-α$^+$IL-2$^+$, TNF-α$^+$IFN-γ$^+$, and IL-2$^+$IFN-γ$^+$) cells and three markers (TNF-α$^+$IL-2$^+$IFN-γ$^+$) compared with CS-pCAIX treated group. These data suggested that L-Myc co-immunization with CAIX-based gene vaccine significantly enhances the induction of antigen-specific multi-functional CD8$^+$ T cells.

3.5 | The functional CD8$^+$ T cells are essential for the anti-tumor effect of CS-pL-Myc/pCAIX vaccine

To determine whether functional CD8$^+$ T cells were critical for the anti-tumor activity induced by CS-pL-Myc/pCAIX vaccine, we performed the depletion of CD8$^+$ T cells using specific mAbs in vivo. After depleting CD8$^+$ T cells, the tumor growth of CS-pL-Myc/pCAIX co-immunized mice was obviously uncontrolled (Figure 6A and B). Similarly, the recovery tumor weight and reduced survival rate were observed in CD8 mAb-treated mice immunized with CS-pL-Myc/pCAIX vaccine (Figure 6C and D). Accordingly, administration of CD8 mAb resulted in the significantly reduced percentages of CD8$^+$ T cells in spleen or TILs from CS-pL-Myc/pCAIX treated mice (Figure 6E). Meanwhile, the decreased percentages of CD8$^+$CD11c$^+$ DCs were also observed in CD8 mAb-treated mice (Figure 6F). Likewise, the tumor-infiltrating CD8 T cells detected by IHC staining were markedly higher in control-treated group than those in CD8 mAb-treated group (Figure 6G and H). These results suggested that CD8$^+$CD11c$^+$ DCs-mediated multi-functional CD8 T cell responses are required for the anti-tumor effects by CS-pL-Myc/pCAIX vaccine.
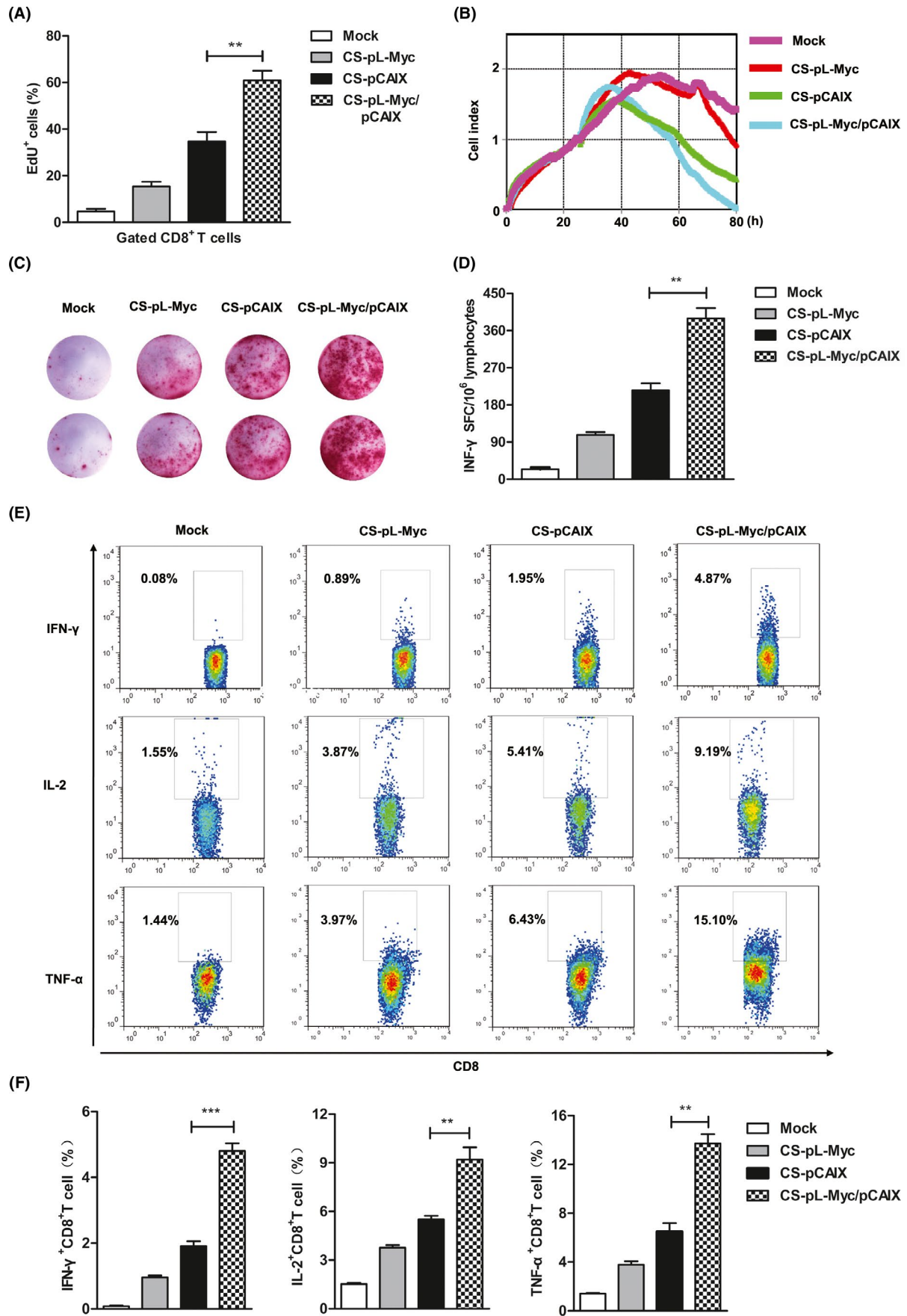
3.6 | CS-pL-Myc/pCAIX vaccine prevents tumor lung metastasis of renal carcinoma

For evaluating the therapeutic effect of CS-pL-Myc/pCAIX vaccine in lung metastasis, the tumor models were established (Figure 7A). 10 days before injecting hCAIX-Renca cells into the tail vein, mice were intramuscularly immunized with variousvaccines, and then repeated vaccination on days 0, 10. The visible metastases of lung were counted after sacrificing mice and removed lungs at day 28 post tumor injection. Compared with CS-pCAIX treatment, CS-pL-Myc/pCAIX treatment significantly reduced the number of lung metastases (Figure 7B and C). H&E staining further confirmed the protective effect of CS-pL-Myc/pCAIX combined immunity in lung metastasis model (Figure 7D). Immunohistochemical staining and flow cytometry showed that the total infiltrating CD8$^+$ T cells of tumor were significantly higher in the CS-pL-Myc/pCAIX group than that in CS-pCAIX group and others (Figure 7E and F). Moreover, multi-functional CD8$^+$ T cell responses were analyzed in vitro. Compared with the control group, CS-pL-Myc/pCAIX group showed that the remarkably increased percentages of CD8$^+$ T cells expressing TNF-α$^+$, IL-2$^+$, or IFN-γ$^+$ in spleen (Figure 7G). A significant increase of IFN-γ-secreting T cells was also observed in CS-pL-Myc/pCAIX group (Figure 7H). Moreover, CTL assay results showed that the effector cells from CS-pL-Myc/pCAIX treated mice produced a stronger killing ability against hCAIX-Renca cells (Figure 7I and J). In short, these results indicated that L-Myc enhanced the ivaccine-induced CD8 $^+$ T cell responses and prevented the tumor growth of lung metastasis in renal carcinoma.

4 | DISCUSSION

Studies have shown that metastatic RCC is sensitive to immunotherapy, which its therapeutic effect, cost, drug resistance, etc are facing challenges.[32] In recent years, immune checkpoint inhibitors and CAR-T studies have been very successful in blood tumors, but they are limited for solid tumor treatment.[33,34] DNA vaccine as part of immunotherapy is designed to encode different antigens to manipulate the resulting immune responses, which is expected to become a breakthrough in relapsed or refractory tumor treatment.[35]

In this study, L-Myc as a vaccine adjuvant was investigated to enhance the DNA vaccine induced anti-tumor immune responses. We speculated that L-Myc was transduced into the body to result in the induction and mature of DCs and CD103$^+$ or CD8$^+$ DCs

(A) EdU⁺ cells (%) — Gated CD8⁺ T cells; groups: Mock, CS-pL-Myc, CS-pCAIX, CS-pL-Myc/pCAIX; ** significance between CS-pCAIX and CS-pL-Myc/pCAIX.

(B) Cell index vs time (h); Mock, CS-pL-Myc, CS-pCAIX, CS-pL-Myc/pCAIX.

(C) Mock, CS-pL-Myc, CS-pCAIX, CS-pL-Myc/pCAIX ELISPOT wells.

(D) INF-γ SFC/10⁶ lymphocytes; Mock, CS-pL-Myc, CS-pCAIX, CS-pL-Myc/pCAIX; **.

(E) Flow cytometry plots for IFN-γ, IL-2, TNF-α gated on CD8; Mock, CS-pL-Myc, CS-pCAIX, CS-pL-Myc/pCAIX.

IFN-γ: 0.08%, 0.89%, 1.95%, 4.87%
IL-2: 1.55%, 3.87%, 5.41%, 9.19%
TNF-α: 1.44%, 3.97%, 6.43%, 15.10%

(F) IFN-γ⁺CD8⁺ T cell (%) ***; IL-2⁺CD8⁺ T cell (%) **; TNF-α⁺CD8⁺ T cell (%) **; Mock, CS-pL-Myc, CS-pCAIX, CS-pL-Myc/pCAIX.

FIGURE 4 CS-pL-Myc/pCAIX co-immunization promotes the tumor-specific CD8 T cell responses. (A) The lymphocytes isolated from spleen of immunized mice were stimulated with CAIX protein (10 μg/ml) in vitro; the percentages of EdU$^+$ cell was assessed in gated CD8 T cells by flow cytometry. (B) RTCA assay were used to measure the CTL activity. (C and D) IFN-γ-secreting T lymphocytes were detected by ELISPOT assay. (E and F) Flow cytometry were performed on splenocytes to assess the proportion of TNF-α$^+$CD8$^+$, IL-2$^+$CD8$^+$, and IFN-γ$^+$CD8$^+$ T cells. The data shown are the representative of three experiments. Data are means ±SD. The different significance was set at**P <.01, ***P <.001

subsets. Accordingly, L-Myc enhanced the ability of DCs for presenting antigens, and L-Myc-mediated DCs induced the stronger induction of antigen-specific CD8$^+$ T cell immune responses. Our results showed that L-Myc could promote the CD103$^+$ or CD8$^+$ DCs mediated CAIX-specific CD8$^+$T cells immune responses that made for better suppression or even degeneration of tumors. Therefore, L-Myc-mediated DCs was required for the start-up CD8$^+$ T cell immune responses, and also supported the hypothesis that L-Myc can be applied to the adjuvant.

DC is regarded as a natural anti-tumor immune mediator that dues to its excellent antigen presentation and naive T cell priming ability.[36] The two important DC subsets CD8α$^+$ DCs and CD103$^+$ DCs, are both classified as cDCs that effectively present antigens in the process of CTL initiation.[37,38] L-Myc expression is necessary for the proliferation activity and function maintenance of the above two DC subgroups. Therefore, we designed the nanoparticle vaccine CS-pL-Myc/pCAIX for the treatment of renal cancer. After subcutaneous immunization, CS-pL-Myc/pCAIX vaccine was taken up and expressed in DCs, thereby enhancing the induction and activation of CD8α$^+$ DCs and CD103$^+$ DCs in vivo. Compared with CS-pCAIX vaccine, CS-pL-Myc/pCAIX vaccine showed the significantly increased proliferation activity and killing efficiency of antigen-specific CD8$^+$ T cells that secreted various cytokines such as IL-2, TNF-α or IFN-γ. Furthermore, the tumor growth was significantly inhibited in CS-pL-Myc/pCAIX co-immunized mice. Likewise, the survival rate of CS-pL-Myc/pCAIX treated-mice was much higher than that of CS-pCAIX-treated mice. Therefore, these data indicated that CS-pL-Myc/pCAIX co-immunization could effectively suppress primary tumor growth.

Our study revealed that the CS-pL-Myc/pCAIX vaccine could enhanced the induction and mature of CD8α$^+$ DCs and CD103$^+$ DCs, and also promoted the proliferation of antigen-specific T cells and the induction of multi-function CD8$^+$ T cells in splenocytes or TILs. These results indicated that an effective CD8 T cell stimulation was induced by the CS-pL-Myc/pCAIX vaccine. Furthermore, the therapeutic effect of CS-pL-Myc/pCAIX vaccine was evaluated through the subcutaneous tumor model and lung metastasis model. L-Myc as an adjuvant combined with CAIX vaccine promoted tumor regression and prolonged mouse lifespan. Of note, administration of CD8 mAb resulted in the deletion of CD8α$^+$ DCs or CD8 T cells in tumor-bearing mice. The therapeutic effect of CS-pL-Myc/pCAIX vaccine was also abrogated in CD8 mAb-treated mice, suggesting that this vaccine function was dependent on CD8α$^+$ DCs-mediated CD8 T-cell immunity. Therefore, the efficacy of CS-pL-Myc/pCAIX vaccine might be required for CD103$^+$DCs, which delivers antigens to the lymphatic organs resident CD8α$^+$ DCs during the anti-tumor CTL response.[39] The analysis of spleen and tumor infiltrating immune cells

in immunized mice showed that CD4$^+$ T cells were not significantly different in each treatment group. But CD4$^+$ helper T cells (Th) were more critical to specific CD8$^+$ CTL immune memory formation and promote memory T cell entering the effective CTL anti-tumor stage.[40,41]

In summary, L-Myc as an adjuvant was successfully applied in anti-tumor vaccine for renal cancer treatment. L-Myc-based vaccine may be served as a therapeutic strategy for primary solid or metastasis tumors.

CONFLICT OF INTEREST

The authors declare no conflict of interest.

ORCID

*Gang Wang* 🆔 https://orcid.org/0000-0001-6020-7263
Junnian Zheng 🆔 https://orcid.org/0000-0003-0208-6410

REFERENCES

1. Siegel RL, Miller KD, Jemal A. Cancer statistics, 2020. *CA Cancer J Clin*. 2020;70(1):7-30.
2. Kim SH, Park WS, Kim SH, et al. Systemic treatments for metastatic renal cell carcinoma: 10-year experience of immunotherapy and targeted therapy. *Cancer Res Treat*. 2016;48:1092-1101.
3. Diaz-Montero CM, Rini BI, Finke JH. The immunology of renal cell carcinoma. *Nat Rev*. 2020;16(12):721-735.
4. Tucker MD, Rini BI. Predicting response to immunotherapy in metastatic renal cell carcinoma. *Cancers*. 2020;12:2662.
5. Scarfo I, Maus MV. Current approaches to increase CAR T cell potency in solid tumors: targeting the tumor microenvironment. *J Immunother Cancer*. 2017;5:28.
6. Zappasodi R, Merghoub T, Wolchok JD. Emerging concepts for immune checkpoint blockade-based combination therapies. *Cancer Cell*. 2018;34:690.
7. Mei Y, Zhao L, Liu Y, et al. Combining DNA Vaccine and AIDA-1 in Attenuated Salmonella Activates Tumor-Specific CD4(+) and CD8(+) T-cell Responses. *Cancer Immunol Res*. 2017;5:503-514.
8. Sun YY, Peng S, Han L, et al. Local HPV Recombinant Vaccinia Boost Following Priming with an HPV DNA Vaccine Enhances Local HPV-Specific CD8+ T-cell-Mediated Tumor Control in the Genital Tract. *Clin Cancer Res*. 2016;22:657-669.
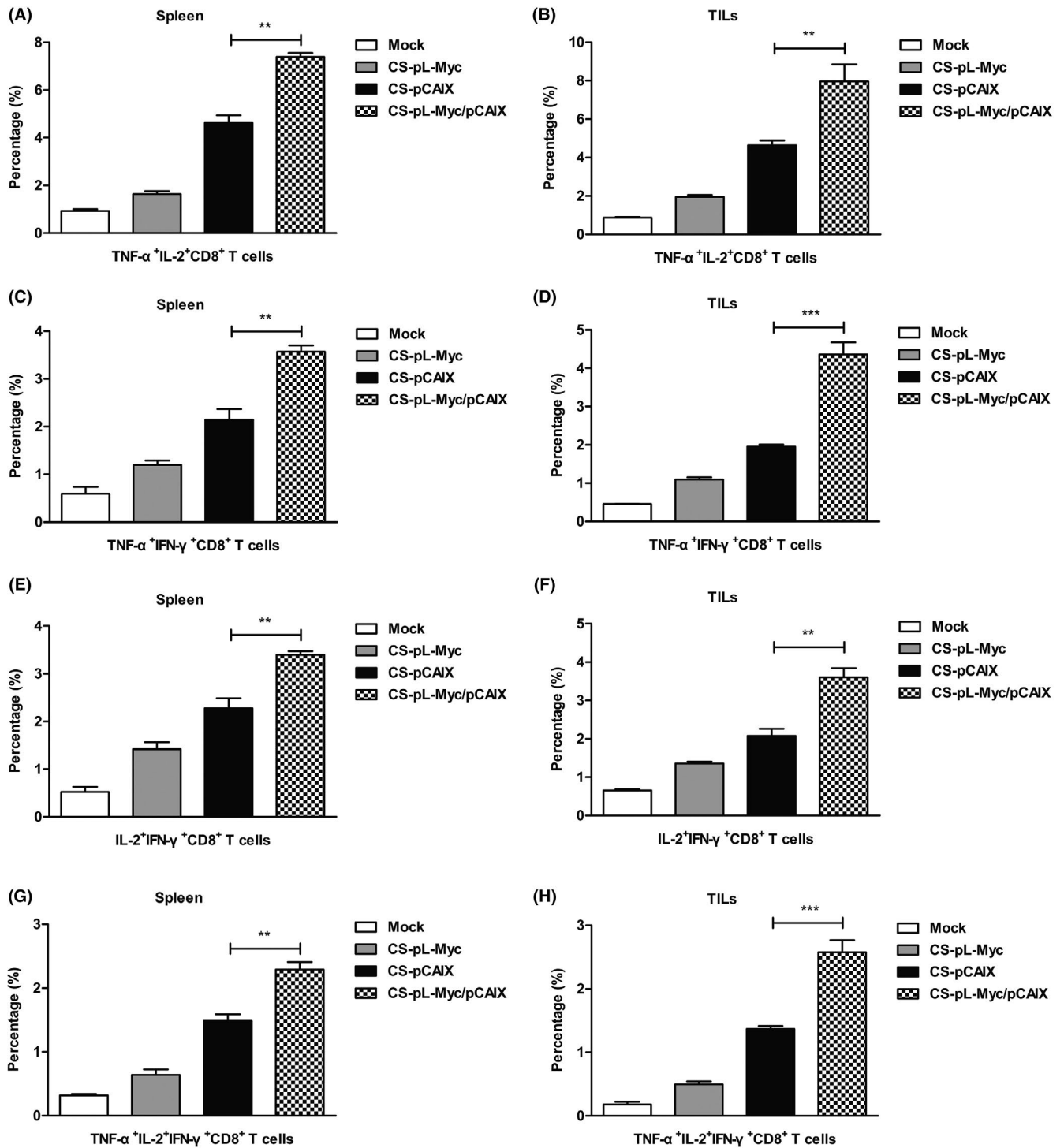
FIGURE 5 CS-pL-Myc/pCAIX co-immunization increased the induction of multi-functional CD8$^+$ T cells. 42 days after the tumor inoculation, splenocytes or TILs from vaccine immunized mice were stimulated in vitro. (A and B) The proportions of t TNF-α$^+$IL-2$^+$CD8$^+$ T cells in spleen or TILs were detected by flow cytometry. (C and D) The percentages of TNF-α$^+$IFN-γ$^+$CD8$^+$ T cells. (E and F) The percentages of IL-2$^+$IFN-γ$^+$CD8$^+$ T cells. (G and H) The proportions of TNF-α$^+$IL-2$^+$IFN-γ$^+$CD8$^+$ T cells. The data shown are the representative of three experiments. Data are means ±SD. The different significance was set at **P <.01, ***P <.001

9. Li L, Petrovsky N. Molecular mechanisms for enhanced DNA vaccine immunogenicity. *Exp Rev Vaccines.* 2016;15:313-329.

10. Stadick H, Stockmeyer B, Kuhn R, et al. Epidermal growth factor receptor and g250: useful target antigens for antibody mediated cellular cytotoxicity against renal cell carcinoma? *J Urol.* 2002;167:707-712.

11. Li G, Feng G, Gentil-Perret A, Genin C, Tostain J. CA9 gene expression in conventional renal cell carcinoma: a potential marker
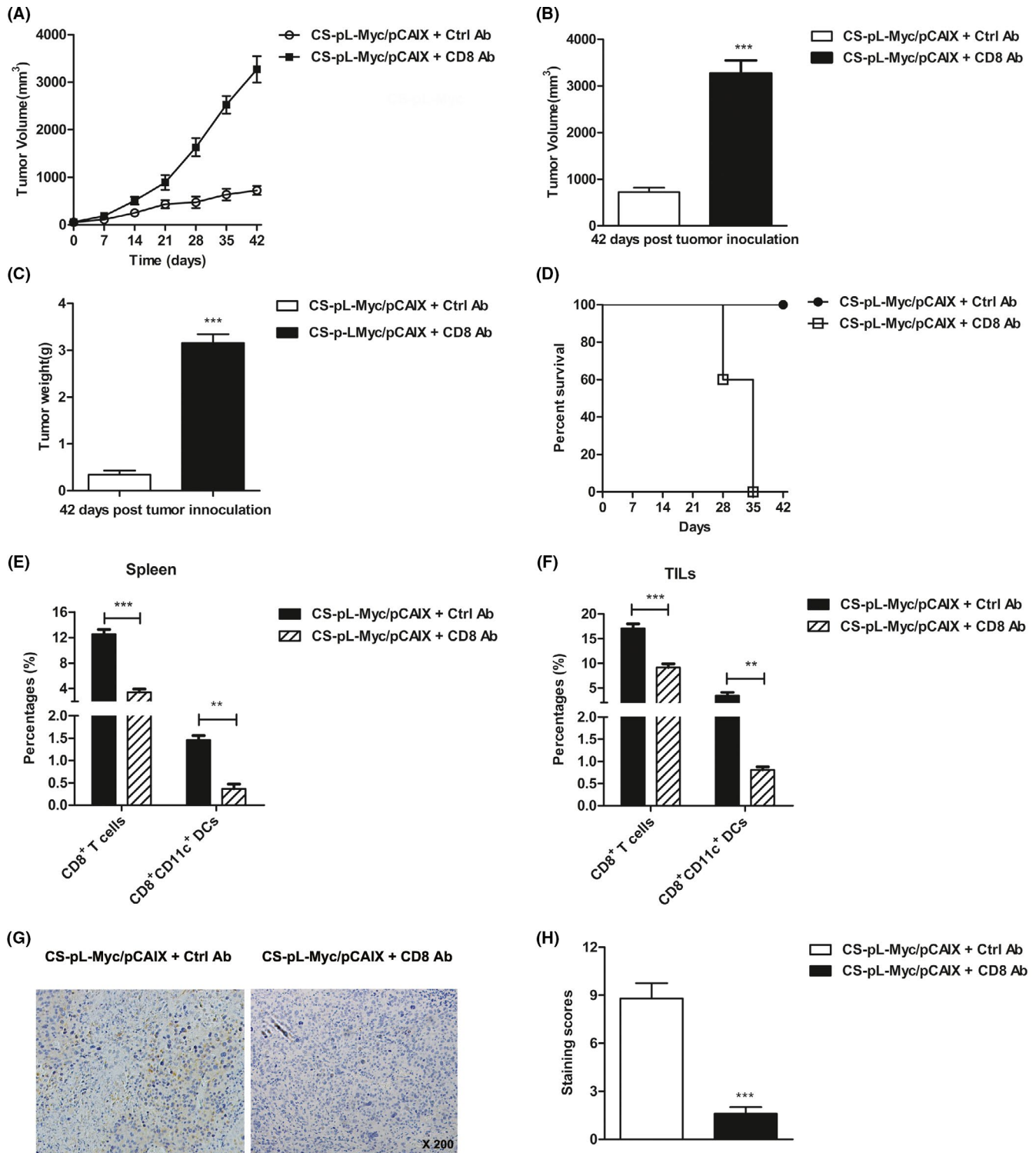
FIGURE 6 Anti-tumor effect induced by CS-pL-Myc/pCAIX vaccine is dependent on CD8 T cell immune responses. In the depleted group of mice, 0.5 mg of anti-mouse CD8 mAb was injected intraperitoneally at day −2, 5 and 12 after vaccination. (A) Tumor progression. (B) Tumor volumes. (C) Tumor weights. (D) Survival rate. (E and F) The proportions of CD8$^+$ T cells and CD8$^+$CD11c$^+$ DCs in spleen or TILs. (G) Immunochemistry staining for CD8$^+$ T cells of tumor tissues (×200 magnification). (H) Staining scores were analyzed in (G). The experiments were conducted with five mice per group. The data shown are the representative of three experiments. Data are means ±SD.**P <.01, ***P <.001

for prediction of early metastasis after nephrectomy. *Clin Exp Metastasis.* 2007;24:149-155.

12. Muselaers S, Mulders P, Oosterwijk E, Oyen W, Boerman O. Molecular imaging and carbonic anhydrase

IX-targeted radioimmunotherapy in clear cell renal cell carcinoma. *Immunotherapy.* 2013;5:489-495.

13. Tostain J, Li G, Gentil-Perret A, Gigante M. Carbonic anhydrase 9 in clear cell renal cell carcinoma: a marker
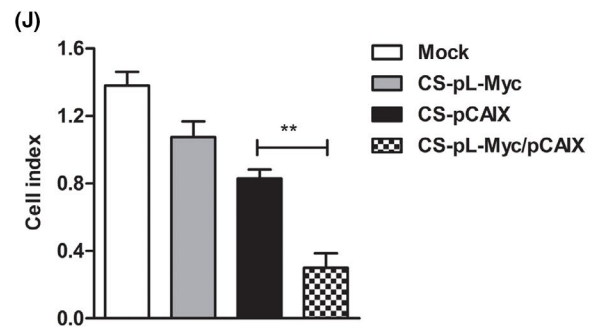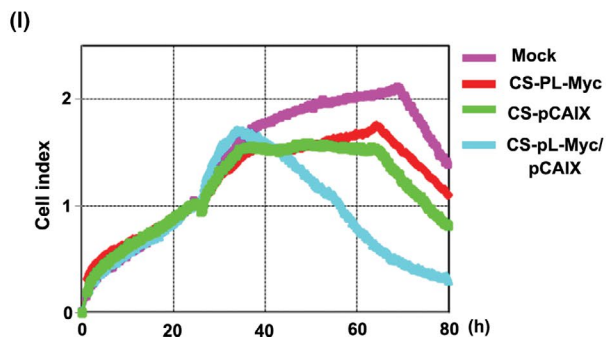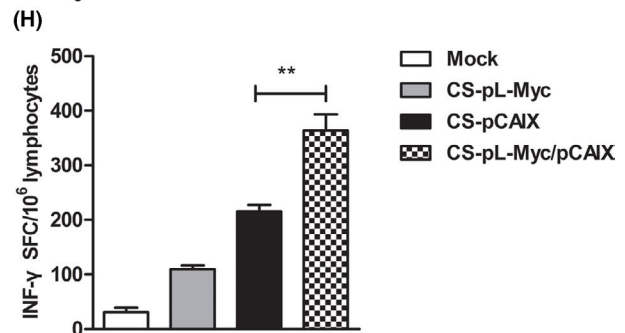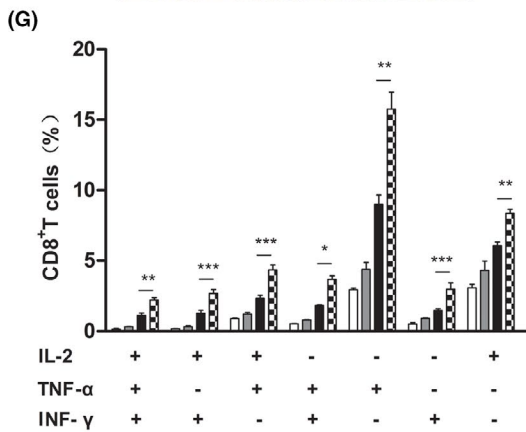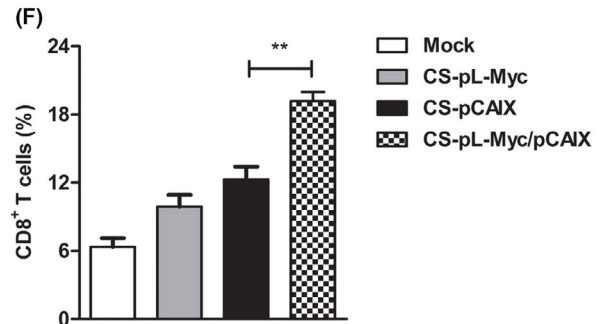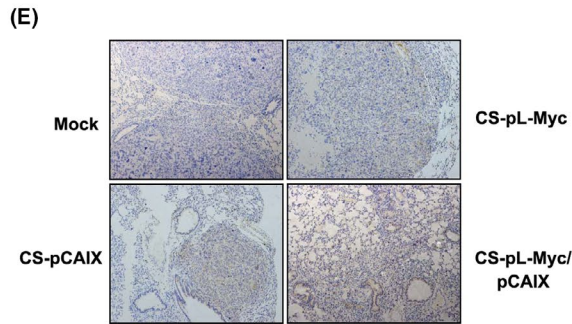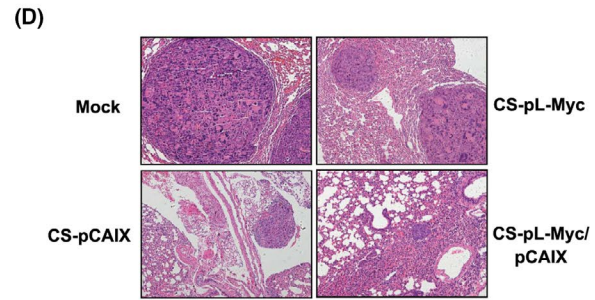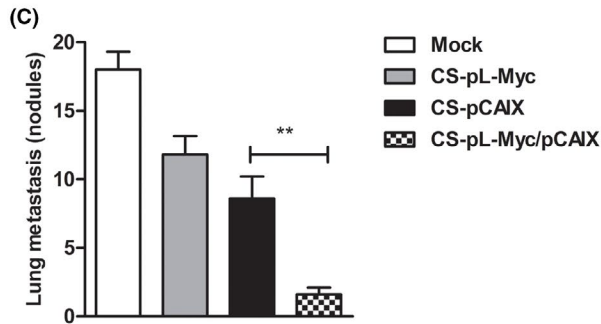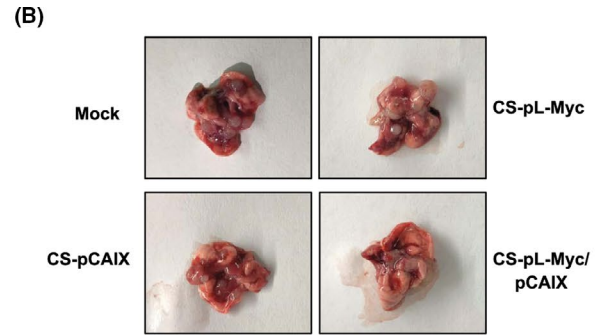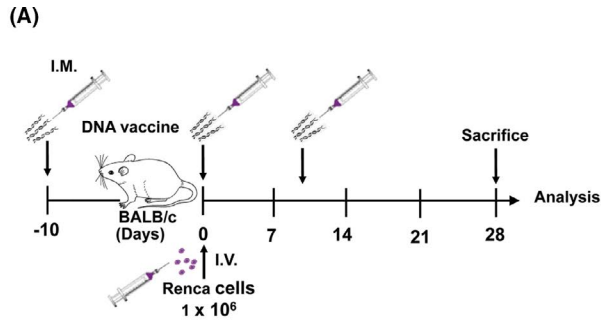
FIGURE 7 CS-pL-Myc/pCAIX co-immunization suppressed the lung metastasis in renal carcinoma model by enhancing multi-functional CD8^{+} T cell responses. (A) Schema of lung metastasis model establishment and experiment. (B) The present images of lung metastasis tumors excised from mice. (C) The numbers of metastatic nodules. (D) Lung tissues performed by H&E staining. (E) CD8^{+} T cells of lung tissues were detected by immunochemistry staining (×200 magnification). (F) The frequencies of CD8^{+} T cells were analyzed by flow cytometry in the lung tumor tissues. (G) Intracellular staining of TNF-α, IFN-γ, and IL-2 of multi-functional CD8^{+} T cells in stimulated splenocytes. (H) CAIX-specific IFN-γ-secreting T lymphocyte cells were quantified by ELISPOT assay. (I) The CTL was detected by RTCA assay. (J) Cell index by RTCA assay were analyzed in (I). The experiments were performed with five mice per group. Data are from one representative experiment of three performed and presented as the mean ±SD. The different significance was set at *P <.05, **P <.01, ***P <.001

for diagnosis, prognosis and treatment. *Eur J Cancer.* 2010;46:3141-3148.

14. Faiena I, Comin-Anduix B, Berent-Maoz B, et al. A phase i, open-label, dose-escalation, and cohort expansion study to evaluate the safety and immune response to autologous dendritic cells transduced with AdGMCA9 (DC-AdGMCAIX) in patients with metastatic renal cell carcinoma. *J Immunother.* 2020;43:273-282.

15. Zhao Y, Wei Z, Yang H, et al. Enhance the anti-renca carcinoma effect of a DNA vaccine targeting G250 gene by co-expression with cytotoxic T-lymphocyte associated antigen-4(CTLA-4). *Biomed Pharmacother.* 2017;90:147-152.

16. Chai D, Shan H, Wang G, et al. Combining DNA Vaccine and AIM2 in H1 Nanoparticles Exert Anti-Renal Carcinoma Effects via Enhancing Tumor-Specific Multi-functional CD8(+) T-cell Responses. *Mol Cancer Ther.* 2019;18:323-334.

17. Li TR, Peng C, Zhong LJ, et al. Effective inhibition of tumor in vivo with a novel DNA vaccine targeting chimeric G250. *Eur Rev Med Pharmacol Sci.* 2020;24:7454-7461.

18. Sun Z, Liu B, Ruan X, Liu Q. An enhanced immune response against G250, induced by a heterologous DNA primeprotein boost vaccination, using polyethyleneimine as a DNA vaccine adjuvant. *Mol Med Rep.* 2014;10:2657-2662.

19. Vissers JL, De Vries IJ, Engelen LP, et al. Renal cell carcinoma-associated antigen G250 encodes a naturally processed epitope presented by human leukocyte antigen-DR molecules to CD4(+) T lymphocytes. *Int J Cancer.* 2002;100:441-444.

20. Tom JK, Albin TJ, Manna S, Moser BA, Steinhardt RC, Esser-Kahn AP. Applications of immunomodulatory immune synergies to adjuvant discovery and vaccine development. *Trends Biotechnol.* 2019;37:373-388.

21. Ingvarsson S. The myc gene family proteins and their role in transformation and differentiation. *Semin Cancer Biol.* 1990;1:359-369.

22. Kc W, Satpathy AT, Rapaport AS, et al. L-Myc expression by dendritic cells is required for optimal T-cell priming. *Nature.* 2014;507:243-247.

23. Lim M, Badruddoza AZM, Firdous J, et al. Engineered nanodelivery systems to improve DNA vaccine technologies. *Pharmaceutics.* 2020;12:30.

24. Naskar S, Koutsu K, Sharma S. Chitosan-based nanoparticles as drug delivery systems: a review on two decades of research. *J Drug Target.* 2019;27:379-393.

25. Kumar S, Garg P, Pandey S, et al. Enhanced chitosan-DNA interaction by 2-acrylamido-2-methylpropane coupling for an efficient transfection in cancer cells. *J Materials Chem.* 2015;3:3465-3475.

26. Chai D, Yue Y, Xu W, Dong C, Xiong S. AIM2 co-immunization favors specific multifunctional CD8(+) T cell induction and ameliorates coxsackievirus B3-induced chronic myocarditis. *Antiviral Res.* 2015;119:68-77.

27. Yue Y, Xu W, Hu L, Jiang Z, Xiong S. Enhanced resistance to coxsackievirus B3-induced myocarditis by intranasal co-immunization of lymphotactin gene encapsulated in chitosan particle. *Virology.* 2009;386:438-447.

28. Bai J, Mei P, Zhang C, et al. BRG1 is a prognostic marker and potential therapeutic target in human breast cancer. *PLoS One.* 2013;8:e59772.

29. Allan RS, Waithman J, Bedoui S, et al. Migratory dendritic cells transfer antigen to a lymph node-resident dendritic cell population for efficient CTL priming. *Immunity.* 2006;25:153-162.

30. Roberts EW, Broz ML, Binnewies M, et al. Critical Role for CD103(+)/CD141(+) Dendritic Cells Bearing CCR7 for Tumor Antigen Trafficking and Priming of T Cell Immunity in Melanoma. *Cancer Cell.* 2016;30:324-336.

31. Levy Y, Thiebaut R, Montes M, et al. Dendritic cell-based therapeutic vaccine elicits polyfunctional HIV-specific T-cell immunity associated with control of viral load. *Eur J Immunol.* 2014;44:2802-2810.

32. Posadas EM, Limvorasak S, Figlin RA. Targeted therapies for renal cell carcinoma. *Nat Rev.* 2017;13:496-511.

33. Alsharedi M, Katz H. Check point inhibitors a new era in renal cell carcinoma treatment. *Med Oncol (Northwood, London, England).* 2018;35:85.

34. Newick K, O'Brien S, Moon E, Albelda SM. CAR T cell therapy for solid tumors. *Ann Rev Med.* 2017;68:139-152.

35. Teixeira L, Medioni J, Garibal J, et al. A First-in-Human Phase I Study of INVAC-1, an Optimized Human Telomerase DNA Vaccine in Patients with Advanced Solid Tumors. *Clin Cancer Res.* 2020;26:588-597.

36. Eisenbarth SC. Dendritic cell subsets in T cell programming: location dictates function. *Nat Rev Immunol.* 2019;19:89-103.

37. Hildner K, Edelson BT, Purtha WE, et al. Batf3 deficiency reveals a critical role for CD8alpha+ dendritic cells in cytotoxic T cell immunity. *Science (New York, NY).* 2008;322:1097-1100.

38. Ginhoux F, Liu K, Helft J, et al. The origin and development of non-lymphoid tissue CD103+ DCs. *J Exp Med.* 2009;206:3115-3130.

39. Fu C, Jiang A. Dendritic cells and CD8 T cell immunity in tumor microenvironment. *Front Immunol.* 2018;9:3059.

40. Umeshappa CS, Nanjundappa RH, Xie Y, Freywald A, Xu Q, Xiang J. Differential requirements of CD4(+) T-cell signals for effector cytotoxic T-lymphocyte (CTL) priming and functional memory CTL development at higher CD8(+) T-cell precursor frequency. *Immunology.* 2013;138:298-306.

41. Ahrends T, Busselaar J, Severson TM, et al. CD4(+) T cell help creates memory CD8(+) T cells with innate and help-independent recall capacities. *Nat Commun.* 2019;10:5531.